High resolution reconstruction of irregularly sampled, aliased measurements

D.J. Verschuur[1], H. Kutscha[2]

[1] *Delft University of Technology, The Netherlands, Email: D.J.Verschuur@tudelft.nl*
[2] *Delft University of Technology, The Netherlands, Email: H.Kutscha@tudelft.nl*

Introduction

In many multi-channel measurement situations it is often not possible to acquire data with sufficiently dense sampled arrays. Furthermore, the measurement locations are not always regularly sampled or may have holes, e.g. due to obstructions. In the field of oil and gas exploration using acoustic signals this is often the case. The objective of exploration seismics is to image the subsurface of the earth based on acoustic reflection measurements made at the surface. A source at the surface emits an acoustic wavefield which propagates through the subsurface. Any inhomogeneity in the earth will cause a part of the downgoing energy to scatter back to the surface, where a line or a grid of receivers is positioned (see Figure 1). The recordings consist of primary and multiple reflections and have, for simple structures, a more or less hyperbolic nature (see Figure 2). Based on wave theory, these reflection measurements can be transformed into an image of the subsurface. Before such an imaging process several preprocessing algorithms have to be applied to the data, e.g. to remove noise and other unwanted energy. These algorithms are usually designed for regularly sampled, alias-free data. Therefore, reconstruction algo-rithms are used to transform the measurements into a regularly sampled, aliasing free dataset. Usually, in these reconstruction algorithms, the assumption is made that the measurements can be efficiently described in a suitable transform domain. Typical examples of such domain transforms are the Fourier transform and the generalized Radon transform. However, due to the non-ideal sampling a straightforward transformation is not possible. Therefore, the reconstruction process is defined as an inversion problem, for which extra constraints have to be included to make the solution unique. In this paper we will give an overview of typical transforms and the involved constraints that can be used to reconstruct measurements onto a user-defined spatial grid.

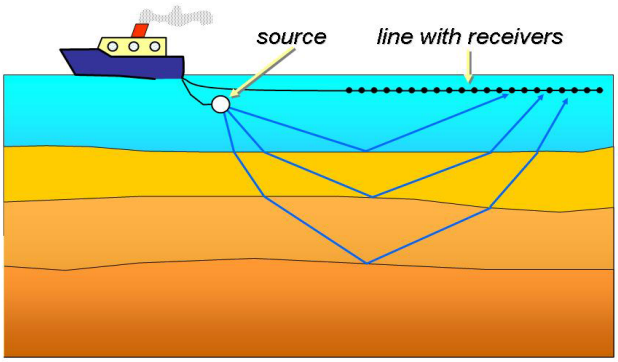

Figure 1: Seismic acquisition in the marine case with a source that emits sound waves and a receiver cable with an array of hydrophones.

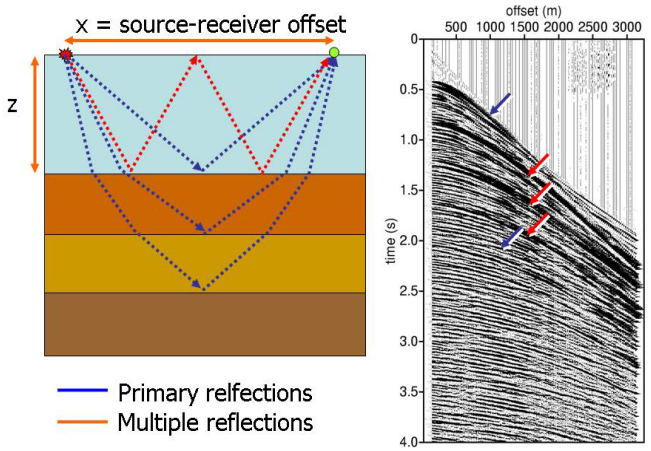

Figure 2: Seismic reflection paths have a hyperbolic nature, as can be observed in the field measurement shown on the right. Blue lines represent primary reflections and the red line is a multiple reflection.

Least-squares Fourier reconstruction

For seismic records reconstruction in the time domain is not necessary. For this reason only spatial reconstruction is addressed here. A popular choice is to use the Fourier transform as the basis for data reconstruction. Thus, we want to describe our dataset in terms of plane wave components. The input dataset (space-time recording, such as shown in Figure 2) is transformed to the space-frequency domain with the Fast Fourier Transform (FFT). Here the inversion can be calculated for each frequency separately. The inversion problem we want to solve is formulated in vector notation as:

$$\mathbf{p} = \mathbf{A}\tilde{\mathbf{p}} + \mathbf{n}\,, \tag{1}$$

with the elements defined as:

$$\begin{aligned} p_n &= p[n\,\Delta x] \\ A_{nm} &= \frac{\Delta k}{2\pi} e^{-j\,m\,\Delta k\,n\,\Delta x} \\ \tilde{p}_m &= \tilde{p}[m\,\Delta k] \quad . \end{aligned} \tag{2}$$

Here $\mathbf{p}$ is the monochromatic data vector in the spatial domain and $\tilde{\mathbf{p}}$ the model vector in the wavenumber domain for respectively one frequency. $\mathbf{A}$ is the inverse Fourier transform matrix, Δx the space sampling and Δk the wavenumber sampling. Energy outside the spatial bandwidth used in the inversion is accounted by the noise term $\mathbf{n}$. After the data were reconstructed for each frequency the space-frequency matrix is transformed back to the space time domain and the reconstruction is evaluated there. For uniform sampling without gaps the total number of traces (N_{tr}) and the total number of wavenumber components (N_k) are equal. In our case the data vector has less entries

(reduced by the number of gaps) than the model vector. Trying to solve the system of equation (1) without any restriction would produce an infinite number of solutions. Thus, certain constraints need to be used. Usually, the solution which has the minimal model norm is chosen. The resulting constrained system has only one solution.

In general the objective of Fourier Reconstruction is to minimize the following quantity:

$$J = \left\| \mathbf{C}_n^{-\frac{1}{2}} (\mathbf{p} - \mathbf{A}\tilde{\mathbf{p}}) \right\|_2^2 = \frac{1}{c^2} \left\| \mathbf{W}^{\frac{1}{2}} (\mathbf{p} - \mathbf{A}\tilde{\mathbf{p}}) \right\|_2^2 , \qquad (3)$$

where $\|\tilde{\mathbf{p}}\|_2^2$ is the L_2 norm of $\tilde{\mathbf{p}}$. The noise covariance matrix can be expressed (Duijndam et al., 1999) as $\mathbf{C}_n = c^2 \mathbf{W}^{-1}$, where c is a constant. The data weighting matrix $\mathbf{W}$ is a diagonal matrix with the diagonal elements defined as $W_{nn} = \Delta x_n$ and is normalized such that $\sum \Delta x_n = 2\pi / \Delta k$. The minimum of equation (3) is obtained by the least-squares estimator:

$$\tilde{\mathbf{p}} = (\mathbf{A}^H \mathbf{W} \mathbf{A})^{-1} \mathbf{A}^H \mathbf{W} \mathbf{p} . \qquad (4)$$

In our case the inverse problem is ill-conditioned due to the lack of information in the missing traces. Thus, the inversion has to be regularized. Here we use damped least squares minimization:

$$J = \frac{1}{c^2} \left\| \mathbf{W}^{\frac{1}{2}} (\mathbf{p} - \mathbf{A}\tilde{\mathbf{p}}) \right\|_2^2 + \frac{1}{\sigma_{\tilde{p}}^2} \|\tilde{\mathbf{p}}\|_2^2 , \qquad (5)$$

where $\sigma_{\tilde{p}}^2$ is the a priori model variance (Zwartjes, 2005). The second term in equation (5) is the restriction on the Euclidean model norm. The minimum of this objective function is derived as:

$$\tilde{\mathbf{p}} = (\mathbf{A}^H \mathbf{W} \mathbf{A} + \lambda \mathbf{I})^{-1} (\mathbf{A}^H \mathbf{W} \mathbf{p}) , \qquad (6)$$

with the damping term $\lambda = c^2 / \sigma_{\tilde{p}}^2$. Here the estimator $\tilde{\mathbf{p}}$, which solves equation (5), is the model vector that explains the data best for certain wavenumbers (band limitation) and coevally has the smallest values. This solution is often referred to as Fourier reconstruction with minimum norm (FRMN). The influence of the constraint can be varied by the damping term λ.

Note, that this represents the commonly used damped least-squares solution (especially when $\mathbf{W} = \mathbf{I}$, where $\mathbf{I}$ is the unity matrix). One should realize that by taking this solution actually means assuming a minimum energy norm on the model space parameters. After the model vectors have been estimated the data are generated on the uniform grid. We refer to Tarantola (1987) for a detailed discussion of inverse theory. Also see Duijndam et al. (1999) and Zwartjes (2005) for further information on FRMN.

In Figure 3c an example of FRMN is shown for the case of two plane wave events (Figure 3a), which have been severely decimated in their spatial sampling (Figure 3b).

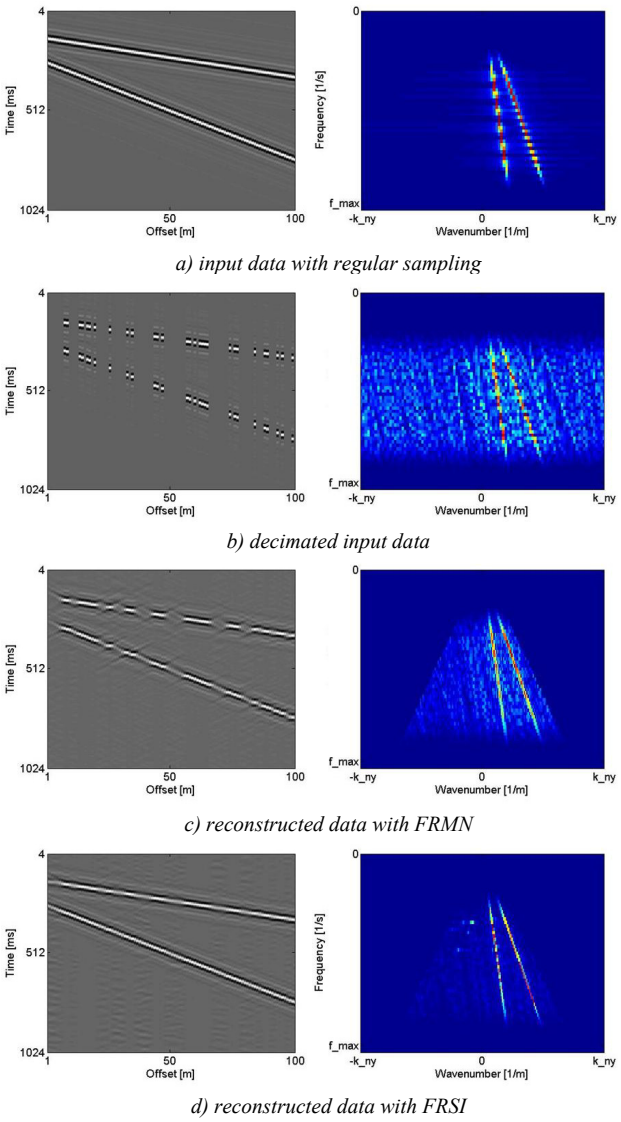

a) input data with regular sampling

b) decimated input data

c) reconstructed data with FRMN

d) reconstructed data with FRSI

Figure 3: Data reconstruction example of irregularly sampled data (b), obtained from decimating a regularly sampled dataset with two plane wave events (a). c) Damped least-squares inversion result (FRMN). d) Result obtained by using the Cauchy sparseness norm (FRSI).

Fourier reconstruction with sparseness

As can be observed in Figure 3c, a proper reconstruction quality of the minimum norm least-squares inversion process is obtained for small gaps only. For the large gaps, the minimum norm constraint enforces the reconstructed wavefield to have small values inside the gaps. Note, however, that the data match is close to perfect (i.e. the reconstructed data resembles the original data at the measurement locations). Thus, to improve the reconstruction quality for the larger gaps, the minimum norm assumption needs to be replaced by another constraint. A popular choice for this is a sparseness constraint. The rationale behind this constraint is that we assume that we need only a limited number of non-zero model domain components (in our case Fourier components) to describe our input data.

For Fourier reconstruction using sparse inversion (FRSI), the following objective function is minimized:

$$J = \frac{1}{c^2}\left\|\mathbf{p} - \mathbf{A}\tilde{\mathbf{p}}\right\|_2^2 + \sum_k \ln(1 + \frac{\tilde{p}_k^* \tilde{p}_k}{\sigma_{\tilde{p}}^2}) , \qquad (7)$$

where the second term represents the Cauchy weighting (see e.g. Zwartjes and Gisolf, 2007). Note that this weighting is data-dependent, such that solving equation (7) becomes a non-linear problem, which is typically carried out by an iterative solver (e.g. a Conjugate Gradient scheme). In each iteration, the model space parameters of the previous iteration are used to construct the least-squares solution:

$$\tilde{\mathbf{p}} = (\mathbf{A}^H \mathbf{A} + \mathbf{S})^{-1} \mathbf{A}^H \mathbf{p} , \qquad (8)$$

where **S** is a diagonal matrix with the elements defined as:

$$S_{kk} = \lambda \frac{1}{1 + \frac{\tilde{p}_k^* \tilde{p}_k}{\sigma_{\tilde{p}}^2}} . \qquad (9)$$

Figure 3d shows the result for of this approach applied to the decimated input data in Figure 3b. Note that the reconstruction has greatly improved compared to the FRMN result. Furthermore, note that indeed the Fourier domain has become much sparser: only the wavenumber components belonging to the two plane events have been emphasized.

Extension to parabolic Radon

From Figure 2 it is clear that in seismic measurements the assumption that the observed responses can be represented by a small number of plane wave comoponents is not true in general. Especially because of the curved nature of the reflection events, a different representation can be more effective. Therefore, it has been proposed to use parabolas as the basis functions. If the seismic measurements are sorted in the so-called common midpoint (CMP) gather domain as a function of offset (see e.g. Yilmaz, 1987), the resulting measurements can be approximated by parabolas with the apex at the zero offset. As a result the parabolas can be described by two parameters: apex time τ and curvature q. The advantage of a parabolic description is that the reconstruction problem can still be defined in the frequency domain (see Hampson, 1986). Basically, all of the previous expressions can be used again, except that the transform matrix **A** need to be redefined as follows:

$$\begin{aligned} p_n &= p[x_n] \\ A_{nm} &= e^{-j\omega m \Delta q x_n^2} \\ \tilde{p}_m &= \tilde{p}[m\Delta k] \end{aligned} \qquad (10)$$

Note that the parabolic Radon transform is not an orthogonal transform, even if the input signal is regularly sampled in x.

Figure 4 demonstrates the least-squares inversion with a minimum norm constraint, as given by equation (6) for the case of a parabolic transform operator. Although the two events map into two small areas in the parabolic Radon domain (Figure 4b), typical smearing effects can be observed due to the fact that the input data is bounded spatially (i.e. edge effects). When imposing a sparseness constraint in the frequency-curvature domain, similar as defined in equation (7), a much better resolution in the Radon domain is obtained, as visible in Figure 5.

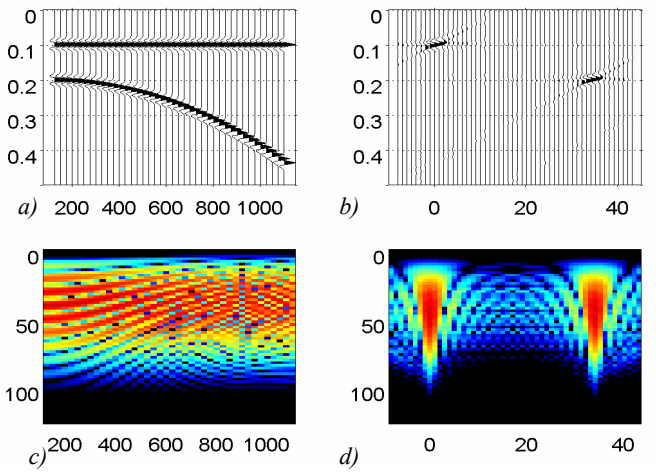

Figure 4: Demonstration of the least-squares parabolic Radon transform using a minimum norm constraint. a) Input data in the space-time domain. b) Transformed data in the curvature-apex time domain. c) Input data in the space-frequency domain. d) Transformed data in the frequency-curvature domain. Note the smearing as observed in the Radon domain (b). (Figure from M. Schonewille)

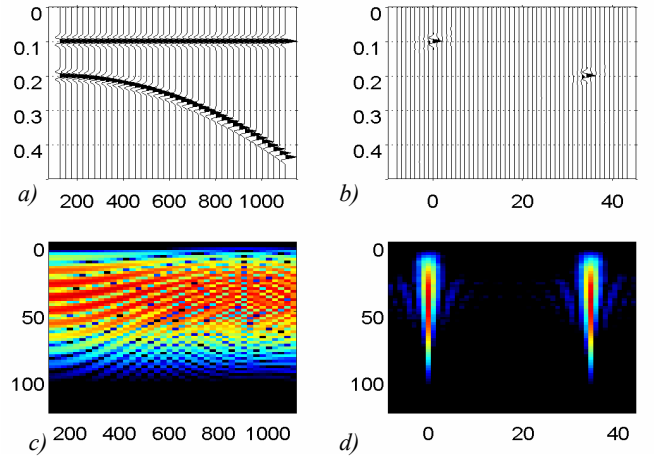

Figure 5: Demonstration of the parabolic Radon transform using a sparseness constraint. a)-d) are similar to Figure 4. Note the high resolution image of the events in the Radon domain (b,d). (Figure from M. Schonewille)

One application of the high-resolution parabolic Radon transform is to separate events with (slightly) different curvatures. This is desired if we want to remove multiple reflections from the seismic measurements. The multiple reflections have travelled more into the shallow part of the earth, where propagation velocities are low. Therefore, the multiples can be recognized as events with a stronger curvature compared to primary events with same arrival time, which have travelled in the deeper part of the earth, where velocities are usually higher.

In Figure 6 such an application is demonstrated on a synthetic data gather from an earth model with three reflecting boundaries. The three primary events are indicated in Figure 6a with the arrows. After the high-resolution Radon transform, each event is focused in a very small area (Figure 6b), after which the undesired multiple events, with the larger curvatures, can be removed by muting (Figure 6c). Finally, the result is transformed back into the space-time domain, yielding the desired primary reflections (Figure 6d).

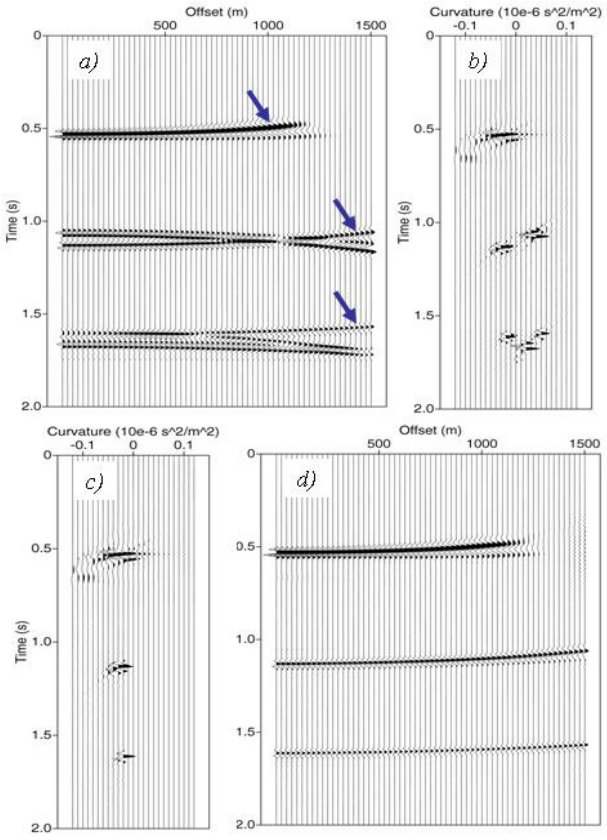

Figure 6: Example of using the high-resolution parabolic Radon transform to separate primaries and multiples. a) Input data gather after an overall curvature correction. The arrows point at the primaries. b) The high-resolution parabolic Radon transform. c) Result of muting the area with the multiple events. d) Reconstructed primaries. Note that the primary reflections are properly reconstructed.

Sparseness in curvature and time

If the spatial sampling becomes too poor, the sparseness constraint in the curvature domain alone is not enough to recover the measurements properly. In that case an additional constraint is included: the data is also sparse in the time domain, meaning that events have an impulsive character. However, to exploit this property, the inversion process needs to be carried out in the time domain, meaning that a decomposition of the huge inversion problem in smaller sub-problems per frequency is not possible. First steps in this direction were already taken by Thorson and Claerbout (1985) and followed-up by Sacchi and Ulrich (1995) and Trad et al. (2003). In van Dedem and Verschuur (2005) this method was used to help reconstructing a severely aliased data that is involved in 3D multiple removal. The following example is from this application, where a well sampled dataset with 10 hyperbolic events (Figure 7a) is severely decimated (Figure 7b). This decimated data becomes the input for an iterative hyperbolic reconstruction process. The initial estimate of the hyperbolic model space (Figure 7d) is obtained by simple summing over all possible hyperbolic trajectories. The resulting estimate has a poor resolution. After applying the sparse inversion process, the estimate of the model space becomes more and more sparse (Figure 7e-g). Finally, the data can be reconstructed with high accuracy to the original dense sampling (Figure 7c).

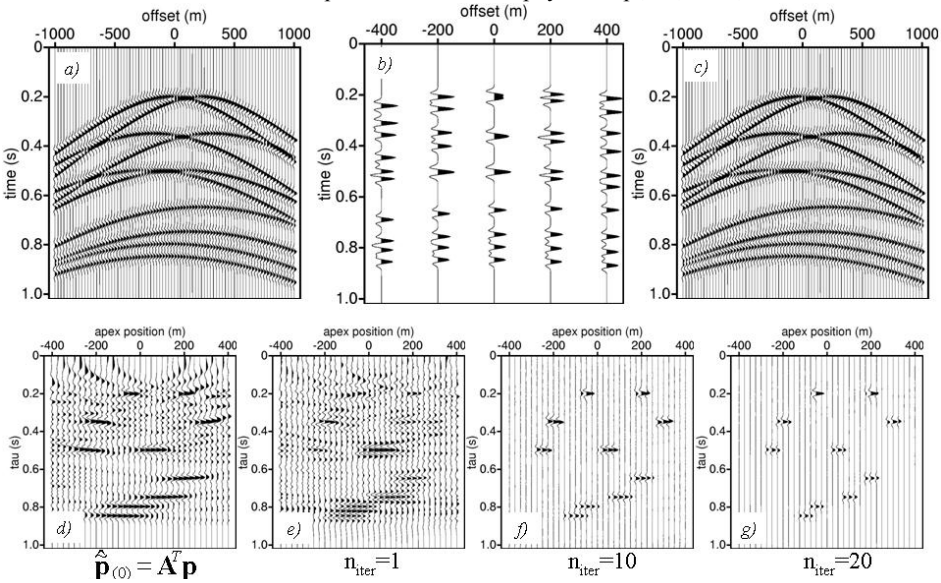

Figure 7: a) Original data with 10 hyperbolic events. b) Decimated input data. c) Reconstructed data with a time domain sparse hyperbolic transform. d) Initial transform domain. e-g) Transform domain after 1, 10 and 20 iterations respectively.

Conclusions

Spatially irregularly sampled and aliased measurements can often be reconstructed with a good quality by choosing the proper transform domain and including a suitable constraint on the model space parameters. In practice, a sparseness constraint is very powerful. The downside of such constraint is that the inversion procedure becomes nonlinear and sometimes cannot be solved independently per frequency.

References

van Dedem, E. J. and D. J. Verschuur, 2005, 3-D surface-related multiple prediction: A sparse inversion approach: Geophysics, **70**, V31–V43.

Duijndam, A. J. W., Schonewille, M. A., and Hindriks, C. O. H., 1999, Reconstruction of band-limited signals, irregularly sampled along one spatial direction: Geophysics, 64, 524–538.

Hampson, D., 1986, Inverse velocity stacking for multiple elimination: Canadian Journal of Expl. Geoph., **22**, 44-55.

Sacchi, M.D., and Ulrych, T.J., 1995, High resolution velocity gathers and offset space reconstruction: Geophysics, **60**, 1169-1177.

Tarantola, A., 1987, Inverse problem theory: Elsevier.

Thorson, J. R. and Claerbout, J. F., 1985, Velocity stack and slant stochastic inversion: Geophysics, **50**, 2727-2741.

Trad, D., Ulrych, T. and Sacchi, M., 2003, Latest views of the sparse Radon transform: Geophysics, **68**, 386-399.

Yilmaz, O., 1987, Seismic data processing, Soc. Expl. Geophys., Tulsa.

Zwartjes, P. M., 2005, Fourier reconstruction with sparse inversion: Ph.D. thesis, Delft University of Technology.

Zwartjes, P. M., and Gisolf, A., 2007, Fourier reconstruction with sparse inversion: Geophys. Prosp., 55, no. 2, 199–221.